

Order–Disorder Phase Transition of Polyelectrolyte Gel–Surfactant Complexes

Shigeo Sasaki* and Shogo Koga

Department of Chemistry and Physics of Condensed Matter, Graduated School of Science, Kyushu University, 33 Hakozaki, Higashi ku, Fukuoka 812, Japan

Received January 26, 2004; Revised Manuscript Received March 17, 2004

ABSTRACT: Small-angle X-ray scattering (SAXS) and elastic measurements were made for polyelectrolyte gel–surfactant complexes (PSCg) of polyacrylate–dodecylpyridinium (PAA–DP) and polyacrylate–cetylpyridinium (PAA–CP) at various NaCl concentrations (C_s). Sharp peaks in the SAXS spectra were observed at C_s lower than 200 mM and disappeared at C_s above 200 mM, where a single broad peak emerged. The sharp peaks of PAA–DP and PAA–CP, respectively, are assigned to the $Pm3n$ cubic and the hexagonal structures, while the single broad peak is due to the correlated pair distribution function of micelles in the liquidlike state. In uniaxially stretching the PSCg, an abnormally large relaxation elastic modulus, of several 10^5 Pa, was observed at C_s below about 200 mM, while a relaxation elastic modulus smaller than 10^3 Pa was observed at C_s above 200 mM. The transitional changes of the steady moduli of the PSCg were also observed at C_s around 200 mM. The relaxation elastic modulus of the PSCg changed transitionally from 200 to 25 kPa with temperature rising from 34 to 36 °C. The results described above clearly demonstrate the existence of an order–disorder or a solid–liquidlike phase transition of the PSCg.

1. Introduction

The crystalline complexes of polyelectrolytes and oppositely charged surfactant molecules have recently attracted a great deal of attention not only because of the fascinating physical conditions used to form them^{1,2} but also because of a possible use of the cationic liposome in the transfection.³ The highly condensed hydrophobic counterions around a polyelectrolyte aggregate and form a micelle due to the hydrophobic attraction. The electrostatic attraction between the micelles and the polyelectrolyte collapses chains.¹ An assembly of the micelles and the collapsed polyelectrolyte chains is called as a polyelectrolyte surfactant complex, PSC. The ordered nanostructures have been often found in the PSC.² The ordered structure can also form in the cross-linked polyelectrolyte gel chain, the complex of which with the surfactant molecule is here denoted by PSCg.

It has been revealed that the high charge density of the polyelectrolyte chain is a necessary condition for forming the ordered nanostructures.^{4,5} The highly condensed state of micelles induced by a high charge density of the chain leads to the ordered nanostructures such as the cubic and the hexagonal structures.⁶ The reduction of the electrostatic interaction with an increase in a salt concentration, C_s , weakens the condensation force and dissolves the PSC.^{7,8} Although much has been revealed about the phase diagrams for the systems of polyelectrolytes, surfactants, and salts in the aqueous media,^{9,10} our knowledge about physical natures of the PSC is very poor. Is the PSC liquidlike or solidlike? For the application to the transfection, it is important to make the liquidlike PSC, which can be injected into biological cells because of its fluidity. The PSC might be solidlike when the polyelectrolyte chain strongly attaches to the micelles, and it might be

liquidlike when the former detaches from the latter. The solidlike structure is rigid but might be elastic, and the liquidlike structure is fluid but might be viscous. To clarify the physical natures, the relation between nanostructures and elastic properties of PSCg is explored by measuring the small-angle X-ray scattering (SAXS) spectra and the relaxation moduli of them.

The measurements of elastic moduli of PSCg are scarce due to experimental difficulties arising from the soft and sticky properties. Recently, we have succeeded in measuring the stress relaxation of PSCg in the aqueous NaCl solutions and found the transitional changing of Young's moduli of PSCg with the NaCl concentration, C_s .¹¹ In uniaxially stretching the cylindrical PSCg, a large stress relaxation, which decays according to a power law of time has been observed for the polyacrylate gel–dodecylpyridinium (PAA–DP) complex in the solution at C_s below 50 mM but not for the gel in the solution at C_s above 100 mM. To clarify which physical state changes at the transition, the C_s -dependent nanostructures and elastic properties of PSCg of PAA–DP and polyacrylate gel–cetylpyridinium (PAA–CP) were investigated by measuring the SAXS spectra and the relaxation moduli. We found that there exist a solidlike phase at low C_s and a liquidlike phase at high C_s in the PSCg and that the former and the latter, respectively, are in the ordered and the disordered states.

2. Experimental Section

The poly(acrylate) gels were prepared by the radical copolymerization^{11,12} in aqueous solution of 1 M acrylic acid and 0.01 M *N,N*-methylenebis(acrylamide) at 60 °C. The gels were synthesized in a glass tube (inner diameter = 0.3 mm) and in a space between two glasses separated by a 1 mm thick spacer of poly(tetrafluoroethylene) sheet. The cylindrical gel was rinsed thoroughly with 1 M HCl aqueous solution, dried, and used to observe the elastic behavior. The plate gel was cut into about a 10 mm square, soaked in a 1 M HCl aqueous solution,

* Corresponding author. E-mail: s-skscc@mbx.nc.kyushu-u.ac.jp.

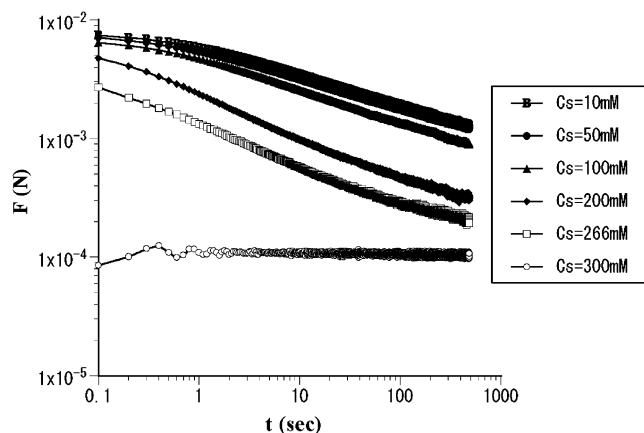


Figure 1. C_s -dependent relaxation of the elastic response to uniaxially stretch of the PAA-CP complexes. A little relaxation is observed for the PSCg at C_s above 300 mM.

dried, and used for the SAXS measurement. Dodecylpyridinium (DP) chloride and cetylpyridinium (CP) chloride were recrystallized from acetone and were used. All chemicals used were of analytical grade. Double distilled water was used.

A detail of the apparatus for monitoring an elastic response of cylindrical gels to the uniaxially elongation has been described elsewhere.^{11,13} The force from 10^{-6} to 3×10^{-2} N was monitored with a time resolution of 1 ms. Two ends of the gel in the dry state were fixed to platinum rings, each of which was connected to a strain sensor and a translational stage through a platinum wire. The gel was immersed into the 1 mM NaOH solution to swell and then the solution was altered with the other solution of a given concentration of NaCl (C_s) and 5 mM surfactant, the pH of which was adjusted between 9 and 10 by adding drops of the NaOH solution. The concentration of the surfactant and NaCl of the solution was not changed by immersing the gel, since the volume of the solution, 100 mL, was much larger than the gel volume, 50 μ L. The equilibration with the solution was confirmed by monitoring the steady tension of the slightly elongated gel. The diameter of the gel, d , was measured with an optical microscope equipped with a computer-aided CCD camera. The elongating length of the gel was adjusted with an accuracy of 1 μ m. The gel was elongated after equilibrating with the solution and the tensile force was recorded with the computer-aided instrument. The gel was elongated (typically several hundreds of micrometers distance) within 0.1 s. The initial tensile force observed, F_i , was found to decay to a steady value, F_s , at t longer than 2000 s after the elongation, as shown in Figure 1. During the measurement, the gel was held in the solution, the temperature of which was controlled with an accuracy of 0.1 $^{\circ}$ C. The natural length of the gel, l_0 , was obtained from an inflection point in a plot of F_s vs the distance between the rings, l . The instantaneous Young's modulus, Y_i , is an elastic response to the deformation at a time just after the elongation, and the steady Young's modulus, Y_s , is an elastic response at an infinitely long time after the elongation. The Y_i and Y_s , respectively, were estimated from the measured elastic forces, F_i and F_s by using the following relations.

$$Y_i = \frac{IF_i}{\pi r_0^2(l - l_0)} \quad (1)$$

and

$$Y_s = \frac{IF_s}{\pi r_0^2(l - l_0)} \quad (2)$$

where r_0 was the radius of the tensile force free gel. The ratio of l to l_0 was typically 1.1. A little relaxation is observed for the PSCg at C_s above 300 mM.

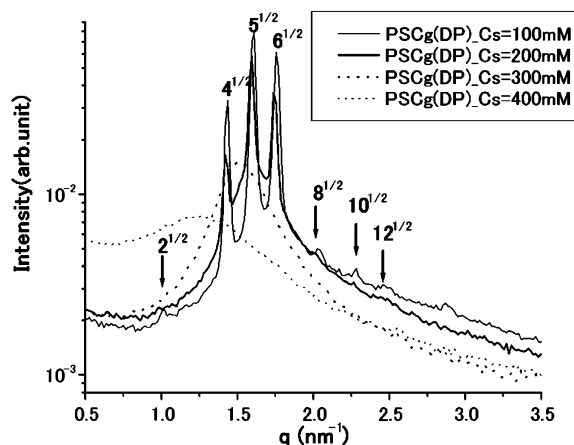


Figure 2. C_s -dependent scattering profiles of the PAA-DP complex at 25 $^{\circ}$ C. Peaks at $C_s = 100$ and 200 mM (solid lines) are indexed assuming a $Pm\bar{3}n$ cubic structure. The broadened peaks at $C_s = 300$ (a broken line) and 400 mM (a dotted line) indicate disordered structures.

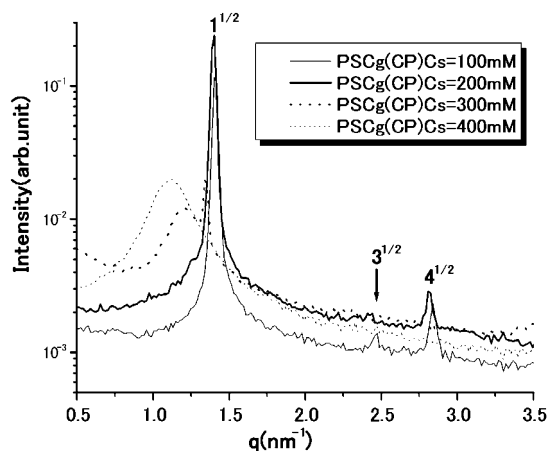


Figure 3. C_s -dependent scattering profiles of PAA-CP complex at 25 $^{\circ}$ C. Peaks at $C_s = 100$ and 200 mM (solid lines) are indexed assuming a hexagonal structure. The broadened peaks at $C_s = 300$ (a broken line) and 400 mM (a dotted line) indicate disordered structures.

The PSCg for the SAXS experiment was prepared as follows. A small amount of 4 N NaOH aqueous solution was added to the dry plate gel in order to fully ionize it. After homogeneously swelling the gel, a small amount of about 1 M surfactant (DPCI or CPCL) aqueous solution, which was the same mole amount of carboxyl group of the gel, was soaked into the gel. Then the gel was immersed into a large amount (about 20 mL) of the aqueous solution of 5 mM surfactant and NaCl of a given concentration. To achieve the equilibration, at which the turbid gels became transparent, the solution containing the gel was held at 60 $^{\circ}$ C for more than a week and at room temperature for more than a day before the measurements.

The SAXS experiments were carried out at 25 $^{\circ}$ C with the SAXS spectrometer of BL45XU-A (RIKEN Beamline I) installed at Spring8 of Japan Synchrotron Radiation Research Institute, Hyogo, Japan, and the SAXS apparatus installed at BL10C of Photon Factory in the Institute of Materials Structure Science (IMSS), High Energy. The observed scattering vectors, q , ranged from 0.07 to 3.5 nm^{-1} .

3. Result

The C_s -dependent SAXS patterns of the PAA-DP and the PAA-CP are shown in Figures 2 and 3. Sharp peaks with a spacing ratio of $\sqrt{2}:\sqrt{4}:\sqrt{5}:\sqrt{6}:\sqrt{8}:\sqrt{10}:\sqrt{12}$ are observed in Figure 2 at C_s less than 200 mM, indicating a cubic structure belonging to $Pm\bar{3}n$ space group.^{5,6} The

Table 1. Salt Concentration Dependence of Characteristic Lengths, a , ξ , and Δ , of PSCg Structures Obtained from the Peaks in SAXS Spectra^a

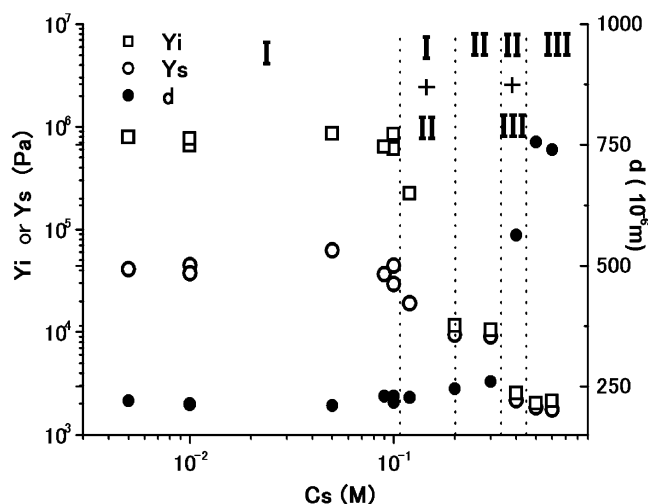
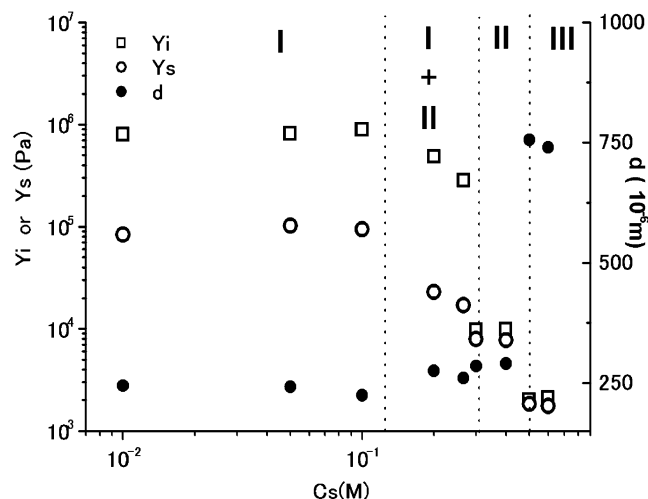
	a (nm)		ξ (nm)		Δ (nm)	
	$C_s = 100$ mM	$C_s = 200$ mM	$C_s = 300$ mM	$C_s = 400$ mM	$C_s = 300$ mM	$C_s = 400$ mM
PAA–DP	8.75 ± 0.03	8.84 ± 0.03	4.10	5.12	17	5
PAA–CP	5.13 ± 0.02	5.17 ± 0.01	5.25	5.63	15	15

^a The a estimated for each peak (100 and 200 mM) is within an error value.

details of the $Pm3n$ cubic structure have been described elsewhere.^{14,15} The Miller indices of corresponding diffraction planes are 110, 200, 210, 211, 220, 310, and 222. Sharp peaks with a spacing ratio of $\sqrt{1}:\sqrt{3}:\sqrt{4}$ are observed in Figure 3 at C_s less than 200 mM, indicating the hexagonal structure,¹⁶ which is a close-packed 2-dimensional array of the rodlike micelles. The Miller indices of corresponding diffraction planes are 100, 110, and 200. The lattice parameters, a of the unit cells are given by $a = 2\pi \sqrt{h^2 + k^2 + l^2} / q_{hkl}$ for the cubic structures and $a = 4\pi \sqrt{h^2 + k^2 + hk} / (\sqrt{3} q_{hkl})$ for the hexagonal structures, where q_{hkl} is a q value of the peak position indexed by hkl .

It is shown in Figures 2 and 3 that a single broad peak emerges at C_s higher than 300 mM instead of the multiple sharp peaks appearing at C_s lower than 200 mM. This indicates the ordered structures dissolve into the disordered structures at C_s between 200 and 300 mM. We can say that the ordered and the disordered states exist in the collapsed PSCg. The single broad peak of SAXS spectra indicates the existence of the liquidlike structure, in which the mean characteristic distance between particles is given by $\xi = 2\pi / q_{\max}$, where q_{\max} is the q value of the intensity maximum position of the single broad peak.¹⁷ The line broadening is related to a mean size of the domain occupied by periodically distributing particles Δ , which can be roughly estimated as $\Delta = \lambda / (\delta\theta \cos\theta/2)$, where λ , θ , and $\delta\theta$, respectively, are the wavelength of the incident beam, the scattering angle of the peak, and the full width (in radians) at half-maximum intensity of the peak.¹⁸ Table 1 shows the C_s dependence of a , ξ , and Δ of the PSCg. It is interesting that the a value and the ξ value significantly increase with C_s . The increase indicates a decrease of the particle's density. The concentrations of the surfactant molecule and the polyelectrolyte have been found to decrease with C_s .¹¹ The added salt to the PSCg weakens the electrostatic force for condensing the polyelectrolyte and the surfactant and decreases their concentrations. It should be mentioned that the averaged particles' distance in the $Pm3n$ cubic lattice, being half of a ¹⁴ for the PAA–DP complex at $C_s = 200$ mM, is longer than ξ for the complex at $C_s = 300$ mM. This indicates the rotation of rodlike particles consisting of the cubic lattice¹⁴ requiring more space than the spherical particles in the disordered structure. Table 1 shows that ratios of Δ to ξ are 1–4 and that a number of the periodically distributing micelles in the disordered PSCg, $(\Delta/\xi)^3$, decrease with the increase in C_s . It is worthwhile to mention that the scattering intensity increases with a decrease of q at q below 0.15 nm^{-1} . This might indicate the existence of a larger structure than the scope of the present studies in the PSCg.

The C_s dependence of moduli, Y_i and Y_s of the PAA–DP and the PAA–CP complexes at 25 °C are shown in

**Figure 4.** C_s dependence of the Young's moduli and the size of PAA–DP complex at 25 °C. Open and close symbols represent the Young's moduli and the size. The phase boundaries are indicated by dotted vertical lines.**Figure 5.** C_s dependence of the Young's moduli and the size of PAA–CP complex at 25 °C. Open and close symbols represent the Young's moduli and the size. The phase boundaries are indicated by dotted vertical lines.**Table 2. Values of C_s , Y_i , $Y_i - Y_s$, and d Characterizing Regimes I, II, and III**

		C_s (mM)	Y_s (Pa)	$Y_i - Y_s$ (Pa)	d (μm)
PAA–DP	I	0–120	4×10^4	7×10^5	220
	II	200–350	9×10^3	1×10^3	250
	III	450–4000	2×10^3	2×10^2	750
PAA–CP	I	0–140	1×10^5	7×10^5	230
	II	300–450	8×10^3	2×10^3	280
	III	450–4000	2×10^3	2×10^2	750

Figures 4 and 5, which also show the C_s dependence of diameters, d of the cylindrical gels. The Y_s values, the differences between Y_i and Y_s , and the d values characterize three regimes, I, II, and III, as shown in Table 2. It is obvious from the C_s dependence of d that regimes I and II are in the collapsed state of polyelectrolyte chain and that regime III is in the swollen state. Table 2 shows that the ratio of the relaxation modulus, $Y_i - Y_s$, to Y_s drastically decreases with a change from regime I to regime II. The present experiment confirms the existence of two regimes, I and II, in the collapsed state of PSCg, which has been reported for the C_s -dependent moduli of the PAA–DP system elsewhere.¹¹ It should be noted here that the C_s values of regimes I and II

correspond to those of the ordered and the disordered states which are indicated by the SAXS spectra shown in Figures 2 and 3. That is, regimes I and II, respectively, are identified with the ordered and the disordered states. The present experiment reveals that the relatively high Y_i and Y_s values and the extremely high relaxation moduli in regime I are related to the ordered nanostructures.

4. Discussions

The C_s -dependent SAXS spectra shown in Figures 2 and 3 demonstrate that the ordered structure in regime I melts in regime II. The large difference between Y_i and Y_s (an order of 7×10^5 Pa) observed in regime I is considered to be related to the elasticity of ordered nanostructures. It is interesting to find out that the values of $F_i - F_s$ are more than 7 times of the F_s values in regime I, as shown in Table 2, and that the elastic force relaxations $F(t)$ shown in Figure 1 can be approximately described by¹¹

$$F(t) = (F_i - F_s)\{\alpha_1 \exp(-t/\tau_1) + (1 - \alpha_1)(1 + t/\tau)^{-\beta}\} + F_s \quad (3)$$

or

$$F(t) = (F_i - F_s) \exp(-t/\tau_1)^\beta + F_s \quad (4)$$

Equation 3 can be partly explained by a gel model consisting of dangling chain ends with topological constraints in the condensed networks¹³ Equation 4, the modified Kohlrausch–Williams–Watt (KWW) equation,¹⁹ has been frequently used to describe relaxation phenomena, while the physical mechanism of the relaxation is not clear. It should be noted that this behavior is very similar to the elastic relaxation of the liquid crystalline elastomer.²⁰ The elastic properties observed for the PSCg in the ordered state might have features similar to that of the liquid crystalline elastomer. The uniaxial stretch of the liquid crystalline elastomer induces a “polydomain-to-monodomain” transition to form a “single liquid crystalline elastomer”.²¹ The orientation of ordered structures in the PSCg to the stretching direction has been clearly observed for PAA–DP at $C_s = 5$ mM.²² This suggests that the uniaxial stretch of the PSCg can also induce the “polydomain-to-monodomain” transition. A change in the SAXS spectrum of PSCg induced by the stretch ends at several tens of seconds²² after the stretch, which is the same order of time as the elastic relaxation time of PSCg in regime I. The coincidence between the relaxation times of changes in the elasticity and the nanostructure strongly indicates that the elastic modulus of the PSCg relaxes with the change from the “polydomain”-ordered structure to the “monodomain”-ordered structure, which might be induced by the dangling chain movement in the condensed networks.¹³

It should be mentioned that the length of the PAA–DP gel stretched in regime I was shortened to restore the gel length to the natural length, l_0 , after releasing the gel from the stress. The deformed network in the cubic structure, which experiences the “polydomain-to-monodomain” transition, seems to take spontaneously the original conformation of the nonstretch gel. The uniaxially stretched conformation of the network is not stabilized by the “monodomain” cubic structure. The time for restoring the gel length to l_0 , however, was

longer than 10 h, which was much longer than the stress relaxation time of the stretched gel. The pathway to restore the chain conformation in regime I is different from the reverse of the pathway to stretch the chain. This might be caused by the “polydomain-to-monodomain” transition of the structure. It should be noted that the stretched PAA–CP gel in regime I did not restore the original natural length at even 2 months after releasing the gel from the external stress. The uniaxially stretched conformation of the network chain in the “monodomain” hexagonal structure is stabilized by the reoriented rodlike micelles to the stretching direction. The PAA–CP gel in regime II, however, restored the original natural length within 1 h after releasing the gel from the external stress. This indicates that the micelles in the PAA–CP gel in regime II are rather spherical than rodlike. The PAA–CP gel stretched in regime I can be annealed in regime II. Therefore, the experiments for obtaining the stress relaxation data of the PAA–CP gel shown in Figures 1 and 5 were made for the gel which experienced regime II beforehand and was set in the given condition.

Figures 4 and 5 show that the relaxation stress in regime I is more than 2 orders of magnitude greater than that in regime II. The differences between regimes I and II as mentioned above and in the previous paragraph can be explained by the gel chains contacting with the surfaces of micelles in regime I and disconnecting from them in regime II. The extremely low rate of the conformational change of the chain and the extremely high stress of the chain are caused by very high activation energy for the detachment of the polyelectrolyte chains from the micelles. The Monte Carlo simulation of polyelectrolyte adsorption on a charged particle²³ has predicted that adsorbed amounts of short polymer chains in the aqueous salt solution suddenly decrease with an increase in C_s at C_s about 100 mM, which is thought to be a critical C_s for the transition from the regime I to the regime II, $C_s^{I \rightarrow II}$. According to the simulation,²³ the chains detach completely from the micelles at C_s above a few hundreds mM, which is considered to correspond to a critical C_s for the transition from the regime II to the regime III, $C_s^{II \rightarrow III}$.

The spectrum reflects the local structure and the elasticity reflects the bulk property. The percolation of disordered structure through the PSCg leads to the elasticity of the disordered body, even when the ordered structures exist in the PSCg. The ordered structures in this case are distributed as like archipelagoes in the sea of the disordered structure. This is observed in the results for the PAA–DP complex at $C_s = 200$ mM: the SAXS spectrum indicating the existence of the ordered structure, as shown in Figure 2, and the elastic property indicating the disordered regime II, as shown in Figure 4. The same type of discrepancy between the SAXS spectrum and the elasticity is also observed for the PAA–CP complex at $C_s = 300$ mM, which yields a sharp peak at $q = 1.34 \text{ nm}^{-1}$ in the SAXS spectrum indicating the ordered structure, as shown in Figure 3, and the Y_i and Y_s values indicating the disordered regime II, as shown in Figure 5. The decrease of the Y_i and the Y_s values with C_s in regime I + II shown in Figures 4 and 5 indicates that a size of the disordered domain in the PSCg increases with C_s . The disordered structure could be distributed in the percolating ordered structure and emerge a broad diffuse scattering spectrum in the background of sharp peaks, as observed in Figure 2.

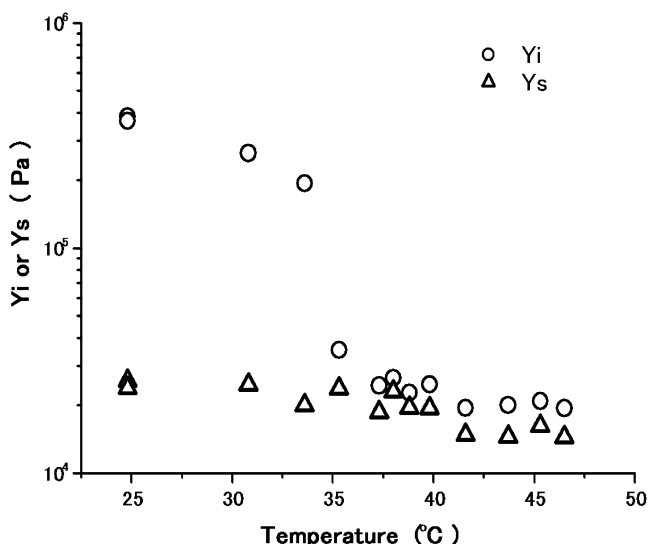


Figure 6. Temperature dependence of the Young's moduli of the PAA-DP complex at $C_s = 95$ mM.

The regime II + III seen in Figure 4 is a coexistence regime of the collapsed and the swollen states. The studies on the binding isotherm of PAA-DP system have revealed the coexistence of the collapsed and the swollen states in PSCg.¹² The existence of the regime II + III indicates a very small difference between the free energies of the swollen chain and the collapsed chain, which is detached from the micelle. The coexistence of the collapsed and the swollen states in one polyelectrolyte chain has been also realized as a pearling structure of the complex of one DNA molecule with histone H1.²⁴ The free energy required to make an interface between the swollen and the collapsed states on one polyelectrolyte chain should be smaller than the thermal free energy.

The order-disorder transition of PSCg with a change of temperature have been observed.²⁵ In raising temperature, the activated motion of the alkyl chains of surfactant molecules due to the increased thermal energy shortens their effective length to decrease a and disappears the ordered structures.²⁵ The mechanism of the temperature driving order-disorder transition of the PSC is considered to be slightly different from the salt driving order-disorder transition, which is due to the decrease in the concentration of the surfactant molecule inside PSC C_{Su}^{+in} ,¹¹ since the a value in regime I increases as C_s approaches $C_s^{I \rightarrow II}$,²² whereas it decreases as the temperature approaches the transition temperature.²⁵ To elucidate the temperature effect on the elastic properties of the PSCg, the elastic relaxation of PAA-DP at $C_s = 95$ mM, and the concentration of the surfactant molecule outside PSC, $C_{Su}^{+out} = 5$ mM was measured with increasing temperature. Figure 6 shows the temperature dependence of the elastic moduli, Y_i and Y_s . A transition is observed at a temperature between 34 and 36 °C. The Y_i value changes abruptly from 200 to 25 kPa, while the Y_s value hardly changes with temperature, as shown in Figure 6. The strength of the electrostatic interaction between the ionized chain and the counterion of micelle is not so much affected by the temperature change. The thermal energy activates the motion of the alkyl chains of surfactant and changes the shape of the micelle. The ellipsoid micelles in the cubic structure of $Pm\bar{3}n$ space group^{14,15} might change to spherical ones at the transition temperature.

The difference between Y_i and Y_s , the relaxation elastic modulus at a temperature below the transition temperature, is 2 orders of magnitude higher than that at a temperature above the transition. This indicates that the polyelectrolyte chain attaches to the micelle at low temperature and detaches from the micelle at high temperature. The thermally activated motion of polyelectrolyte chains and surfactant monomers in the micelle might promote the detachment from each other. The unchangeable Y_s with the order-disorder transition induced by temperature, as shown in Figure 6, is different from the decrease in Y_s with the salt-induced transition, as shown in Figure 4. It should be mentioned here that no change of the gel diameter with temperature was observed during the transition. It is reasonable to say that a small conformational change of the polyelectrolyte chain in the PSCg with temperature induces the small change of the entropy force of chain, Y_s .

It should be mentioned that the $C_s^{I \rightarrow II}$ depends on C_{Su}^{+out} . For the PAA-DP system, the $C_s^{I \rightarrow II}$ has been found to be about 80 mM at $C_{Su}^{+out} = 3$ mM, as reported elsewhere,¹¹ while it is about 120 mM at $C_{Su}^{+out} = 5$ mM, as shown in Figure 4. This is very similar to the situation that the $C_s^{II \rightarrow III}$ increases with the increase in C_{Su}^{+out} .⁷ The C_{Su}^{+in} at thermodynamic equilibrium as a function of C_{Su}^{+out} has not been well clarified, although it has been reported that C_{Su}^{+in} increases with C_{Su}^{+out} .⁴ The detail relation between C_{Su}^{+in} and C_{Su}^{+out} is under investigation.

5. Conclusions

We found a phase transition from the solidlike ordered structure to the liquidlike disordered structure of the polyelectrolyte-surfactant complex system with increases in C_s and temperature by use of SAXS and the elastic measurements. Sharp peaks in the SAXS spectra indicating the ordered structure were observed for the PSCg at C_s lower than 200 mM and a single broad peak indicating the correlated pair distribution function of micelles in the liquidlike state was observed for the PSCg at C_s above 200 mM. An abnormally large relaxation elastic modulus, several 10^5 Pa was observed for the PSCg at C_s below 200 mM, while a relaxation elastic modulus smaller than 10^3 Pa was observed at C_s above 200 mM. The same type of relaxation elastic modulus transition was observed for the PSCg with the change in temperature. The present experiments clearly demonstrate the existence of an order-disorder or solid-liquidlike phase transition of PSCg with C_s and temperature.

Acknowledgment. The SAXS experiments were performed at SPring-8 with the approval of the Japan Synchrotron Radiation Research Institute. The SAXS experiments were also performed under the approval of the Photon Factory Advisory Committee. S.K. is grateful to the Research Fellowship of Japan Society for the Promotion of Science for Young Scientists for partial financial support. The authors were indebted to Dr. M. Sugiyama for his kind help in the SAXS measurements.

References and Notes

- (1) Khandurina, Yu. V.; Dembo, A. T.; Rogacheva, V. B.; Zezin, A. B.; Kabanov, V. A. *Polym. Sci.* **1994**, *36*, 189-194.
- (2) Sokolov, E. L.; Yeh, F.; Khokhlov, A.; Chu, B. *Langmuir* **1996**, *12*, 6229-6234.

- (3) Nabel, G. J.; Nabel, E. G.; Yang, Z. Y.; Fox, B.; Plautz, G. E.; Gao, X.; Huang, I.; Shu, S.; Gordon, D.; Chang, A. E. *Proc. Natl. Acad. Sci. U.S.A.* **1993**, *90*, 11307–11311.
- (4) Zhou, S.; Burger, C.; Yeh, F.; Chu, B. *Macromolecules* **1998**, *31*, 8157–8163.
- (5) Zhou, S.; Yeh, F.; Burger, C.; Chu, B. *J. Phys. Chem. B* **1999**, *103*, 2107–2112.
- (6) Balmbra, R. R.; Clunie, J. S.; Goodman, J. F. *Nature (London)* **1969**, *222*, 1159–1160.
- (7) Sasaki, S.; Koga, S.; Imabayashi, R.; Maeda, H. *J. Phys. Chem. B* **2001**, *105*, 5852–5855.
- (8) Khokholov, A. R.; Kramanenko, E. Yu.; Makhaecva, E. E.; Starodubtzev, S. G. *Macromolecules* **1992**, *25*, 4779–4783.
- (9) Thalberg, K.; Lindman, B.; Bergfeldt, K. *Langmuir* **1991**, *7*, 2893–2898.
- (10) Ilekli, P.; Piculelli, L.; Tournilhac, F.; Cabane, B. *J. Phys. Chem. B* **1998**, *102*, 344–351.
- (11) Sasaki, S.; Koga, S. *J. Phys. Chem. B* **2002**, *106*, 11893–11897.
- (12) Sasaki, S.; Fujimoto, D.; Maeda, H. *Polym. Gels Networks* **1995**, *3*, 145–158.
- (13) Sasaki, S.; Koga, S. *Macromolecules* **2002**, *35*, 857–860.
- (14) Fontell, K. *Colloid Polym. Sci.* **1990**, *268*, 264–285.
- (15) Hansson, P. *Langmuir* **1998**, *14*, 4059–4064.
- (16) Kogej, K.; Evmenenko, G.; Theunissen, E.; Škerjanc, J.; Berghmans, H.; Reynaers, H.; Bras, W. *Macromol. Rapid Commun.* **2000**, *21*, 1226–1233.
- (17) Kogej, K. *J. Phys. Chem. B* **2003**, *107*, 8003–8010.
- (18) Sherrer, P. *Göttigener Nachr.* **1918**, *2*, 98.
- (19) William, G.; Watts, D. C. *Trans. Faraday Soc.* **1971**, *67*, 1323.
- (20) Ortiz, C.; Ober, C. K.; Kramer, E. *J. Polymer* **1998**, *39*, 3713–3178.
- (21) Barclay, G. G.; Ober, C. K. *Prog. Polym. Sci.* **1993**, *18*, 899–945.
- (22) Sasaki, S.; Koga, S.; Sugiyama, M.; Annaka, M. *Phys. Rev. E* **2003**, *68*, 21504–21510.
- (23) Chodanowski, P.; Stoll, S. *Macromolecules* **2001**, *34*, 2320–2328.
- (24) Yoshikawa, Y.; Velichko, Y. S.; Ichiba, Y.; Yoshikawa, K. *Eur. J. Biochem.* **2001**, *268*, 2593–2599.
- (25) Sokolov, E.; Yeh, F.; Khokhlov, A.; Grinberg, V. Y.; Chu, B. *J. Phys. Chem. B* **1998**, *102*, 7091–7098.

MA049829E